Neurobiology of Disease 208 (2025) 106863

Contents lists available at ScienceDirect

Neurobiology of Disease

journal homepage: www.elsevier.com/locate/ynbdi

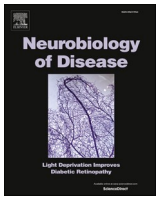

Impaired folate metabolism reshapes auditory response profiles and impairs loudness perception in MTHFR-deficient mice

Hila Sapir [a,1], Ghattas Bisharat [a,1], Hava Golan [b,c], Jennifer Resnik [a,c,*]

[a] Department of Life Sciences, Ben-Gurion University of the Negev, 84105 Beer Sheva, Israel
[b] Department of Physiology and Cell Biology, Ben-Gurion University of the Negev, 84105 Beer Sheva, Israel
[c] Zelman Center for Brian Science Research, Ben-Gurion University of the Negev, 84105 Beer Sheva, Israel

ARTICLE INFO

Keywords:
Auditory processing
2-photon imaging
Folate metabolism

ABSTRACT

Folate metabolism, regulated by methylenetetrahydrofolate reductase (MTHFR), is crucial for proper neurodevelopment, and disruptions—whether due to genetic polymorphisms or maternal nutritional deficits—have been linked to cognitive and behavioral impairments. Notably, MTHFR-deficient mouse models display altered social interaction and auditory communication, hinting at disruptions in auditory-related circuits and prompting the question of whether impaired folate metabolism might also affect sound processing and perception. Here, using two-photon calcium imaging, we show that MTHFR deficiency increases both spontaneous and sound-evoked activity in the auditory cortex and significantly shifts neuronal response profiles, which in turn elevates perceived loudness while reducing sound-level discrimination. These findings underscore the potential role of compromised folate metabolism in driving the atypical auditory responses and may have broader relevance for understanding sensory dysfunction in various neurodevelopmental conditions.

1. Introduction

Folate metabolism has a key role in shaping crucial aspects of brain function, including neuronal growth, synaptic integrity, and plasticity during development (Mattson and Shea, 2003). Within this metabolic pathway, the enzyme methylenetetrahydrofolate reductase (MTHFR) regulates the availability of methyl donors crucial for normal neurodevelopment. Variation in MTHFR function can arise from genetic polymorphisms, maternal nutritional status, or both, creating a gene-environment interaction that may predispose offspring to neurodevelopmental disorders (Boris and Galanko, 2004; Goin-Kochel et al., 2009; Liu et al., 2011; Lewis et al., 2005; Pu et al., 2013). The Mthfr677C > T polymorphism is one of the most widely studied genetic variants in folate metabolism and is characterized by a missense mutation that reduces the enzyme's thermal stability (Lewis et al., 2005; Muntjewerff et al., 2006). This impaired function can lead to elevated homocysteine levels, alter DNA methylation, and disrupt various metabolic processes (Boris and Galanko, 2004; Feng et al., 2009). This polymorphism is relatively common, with frequencies of approximately 20–40 % among many Caucasian populations and potentially higher in certain East Asian groups (Lewis et al., 2005; Muntjewerff et al., 2006). Although commonly examined in the context of neural tube defects (van der Put et al., 1997) and cardiovascular disease (Frosst et al., 1995), the Mthfr677C > T polymorphism has also been linked to neuropsychiatric and neurodevelopmental disorders, including autism spectrum disorder (ASD) (Boris and Galanko, 2004; Goin-Kochel et al., 2009; Liu et al., 2011; Orenbuch et al., 2019; Mohammad et al., 2009) and schizophrenia (Lewis et al., 2005; Feng et al., 2009; Agam et al., 2020). Maternal folate intake can mitigate some of the risks associated with this variant, highlighting the interplay between genetic predisposition, nutritional status, and metabolic homeostasis (Levine et al., 2018; Roza et al., 2010; Zou et al., 2021).

Disruptions in MTHFR activity—whether through maternal deficiencies or offspring-specific polymorphisms—are increasingly recognized for their potential to alter neural circuitry (Lewis et al., 2005; Muntjewerff et al., 2006; Mohammad et al., 2009; Levine et al., 2018; Roza et al., 2010; Zou et al., 2021; Sadigurschi and Golan, 2019). MTHFR-deficient mouse models (Chen et al., 2001), therefore, offer a powerful system to investigate how impaired folate metabolism influences neural activity. MTHFR-deficient mice exhibit elevated glutamate-related proteins and reduced GABA-related proteins in the cortex (Orenbuch et al., 2019)—changes expected to alter basal cortical

* Corresponding author at: Department of Life Sciences, Ben-Gurion University of the Negev, 84105 Beer Sheva, Israel.
E-mail address: resnikj@bgu.ac.il (J. Resnik).
[1] These authors contributed equally to this work.

https://doi.org/10.1016/j.nbd.2025.106863
Received 21 January 2025; Received in revised form 20 February 2025; Accepted 3 March 2025
Available online 7 March 2025

activity and disrupt the normal excitatory-inhibitory balance crucial for sensory processing. Moreover, previous research in this animal model reveals changes in social interaction and auditory communication (Sadigurschi et al., 2023; Gal et al., 2023; Shekel et al., 2021). Notably, mice with maternal or offspring Mthfr deficiency exhibit altered ultrasonic vocalizations (e.g., start/end frequency, duration) (Gal et al., 2023; Shekel et al., 2021), suggesting that both the production and perception of sounds are affected by disruptions in auditory-related circuits. These findings imply that MTHFR-dependent metabolic dysregulation could directly impact the intrinsic properties of the auditory cortex, potentially leading to atypical sound responsiveness—manifesting as hyper- or hypo-sensitivity to environmental stimuli—yet whether there is indeed a change in cortical sound processing remains unclear.

To address this question, we examined auditory cortical responses in MTHFR-deficient and wild-type (WT) mice. We employed calcium imaging to track single-neuron activity in vivo while animals were exposed to noise bursts of varying intensities. Our data reveals that MTHFR deficiency results in increased sound-evoked and spontaneous activity in the auditory cortex, together with shifts in the distribution of response profiles. Our findings implicate deficits in folate metabolism as a critical factor that can increase perceived loudness and reduce sound-level discrimination, offering new insights into how gene-environmental interactions may give rise to the diverse auditory processing phenotypes observed in many neurodevelopmental disorders.

2. Results

To directly assess if MTHFR deficiency causes altered sensory processing in adults, we performed chronic two-photon calcium imaging in the primary auditory cortex (ACtx) of awake, head-fixed MTHFR-deficient mice (Fig. 1a, N = 5 mice, $n = 1809$ cells) that expressed GCaMP6s non-selectively in L2/3 neurons while mice were presented with white noise of varying intensity and compared their cortical sound-evoked responses to WT mice (Fig. 1b, N = 4 mice, $n = 1685$ cells).

2.1. Elevated baseline activity and higher proportion of sound-responsive neurons in MTHFR-deficient mice

Changes in sound-evoked activity can arise from alterations in baseline (pre-sound) activity, post-sound responses, or from shifts in the relationship between these two (Tamamaki et al., 2003; Rudy et al., 2011; Rupert and Shea, 2022; Cauli et al., 1997). To disentangle these possibilities, we first analyzed baseline and post-sound activity separately. We began by assessing baseline cortical activity, analyzing deconvolved spike activity (Pachitariu et al., 2018) in the one-second window preceding sound onset. MTHFR-deficient mice exhibited significantly elevated spontaneous activity compared to WT mice (Fig. 1c t-test $p = 1.6 \times 10^{-12}$).

Having identified elevated baseline activity in MTHFR-deficient mice, we next investigated how this might impact sound responsiveness. Elevated baseline activity can potentially impair the signal-to-noise ratio and reduce the proportion of sound-responsive cells. To test if this was the case, we calculated the percentage of sound-

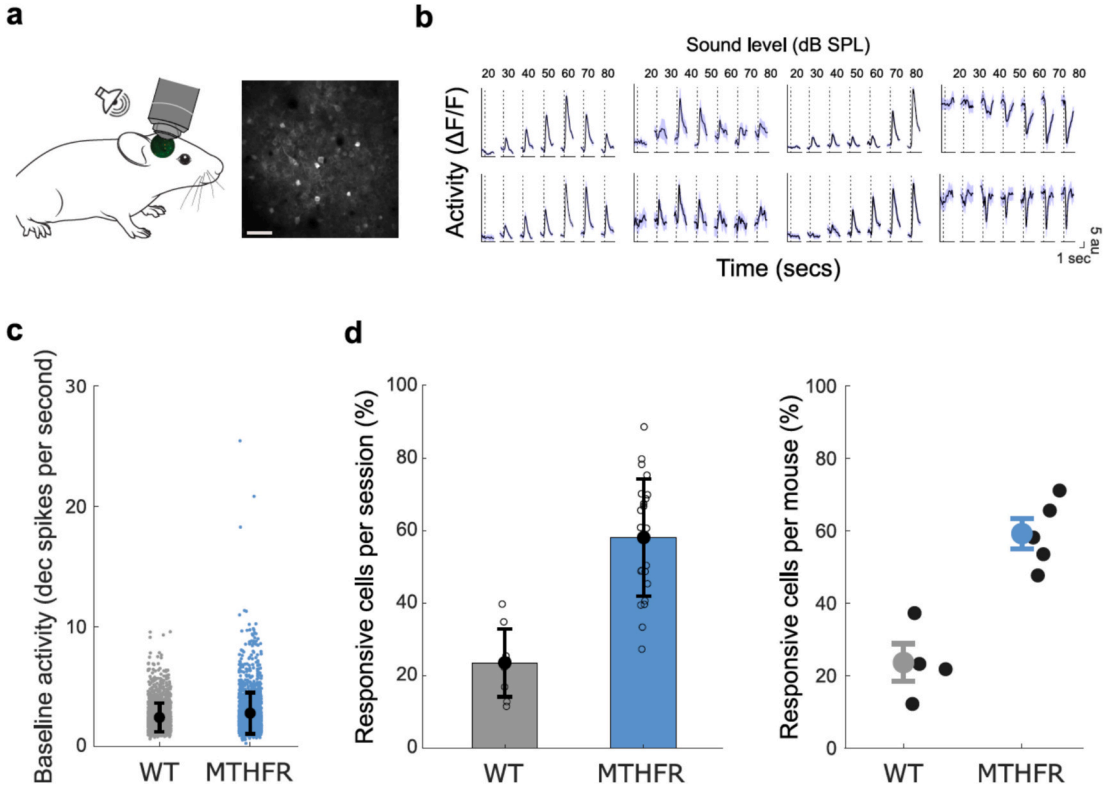

Fig. 1. Elevated baseline activity and higher proportion of sound-responsive neurons in MTHFR-deficient mice
(a) Schematics of two-photon imaging from the primary auditory cortex of awake, head-fixed mice that expressed GCaMP6s non-selectively in L2/3 neurons (WT $n =$ 1685 cells / $N = 4$ mice and MTHFR-deficient mice $N = 5$ mice / $n = 1809$ cells) during sound presentation. Right: Example of imaging plane (scale bar, 50 μm).
(b) Example of sound-evoked activity in WT and MTHFR-deficient mice during white noise presentation at different sound levels (dotted line).
(c) Baseline activity, measured as deconvolved spike activity in the second preceding sound onset, was significantly increased in imaged neurons from MTHFR-deficient mice compared to WT mice (t-test $p = 1.6 \times 10^{-12}$, mean ± se).
(d)Increased percentage of sound-responsive neurons in MTHFR-deficient mice compared to WT mice, when comparing animals (right, t-test $p = 0.011$) or sessions (left, t-test $p = 0.021$). Data are represented as mean ± se.

responsive neurons in both MTHFR-deficient and WT mice. After normalizing post-sound activity for each cell and trial, we did not observe a reduction of sound-responsive neurons in MTHFR-deficient mice. On the contrary, we found a significantly higher percentage of sound-responsive cells compared to WT mice, both when analyzing data at the animal level (Fig. 1d right, *t*-test $p = 0.001$) and session level (Fig. 1d left, t-test $p = 1.4 \times 10^{-06}$).

2.2. Altered sound-level response profiles and increased sound-evoked activity in MTHFR-deficient mice

An increase in the percentage of responsive cells could either reflect a rise in sound-evoked activity per cell or indicate that MTHFR-deficient mice exhibit a similar overall response magnitude, distributed across a larger number of neurons. The combination of elevated baseline activity and a higher proportion of responsive cells suggests the former scenario is more likely. To test this hypothesis, we analyzed the activity of individual sound-responsive cells from WT ($n = 472$) and MTHFR-deficient ($n = 1054$) mice in response to varying levels of white noise.

Given the substantial heterogeneity in sound-level encoding across auditory cortical neurons (Clayton et al., 2024; Wu et al., 2006; Phillips et al., 1995; Schreiner et al., 1992), we first categorize neurons based on their sound-level response profiles. To do so, we applied K-means clustering to the normalized ΔF/F activity of sound-responsive cells, unbiasedly identifying four main response profiles (Fig. 2a): saturated cells (low-threshold, saturating responses), high-threshold cells (monotonic increases at higher sound levels), non-monotonic cells (responses peaking at intermediate levels), and suppressed cells (showing reduced activity at intermediate sound levels).

In WT mice, the proportions of these cell types aligned with values documented in the literature (Clayton et al., 2024), with monotonic cells (high-threshold + saturated) comprising 35.6 and 29.4 % of the cells (Fig. 2a top, $n = 168 + 139$). Non-monotonic cells comprising 27.5 % ($n = 130$) and suppressed cells comprising 7.4 % ($n = 35$). In contrast, MTHFR-deficient mice exhibited a significantly altered distribution (Fig. 2a bottom, chi2 = 141.3 $p = 1.8 \times 10^{-30}$). These mice displayed a markedly higher proportion of suppressed cells (30.2 %, $n = 318$), a reduced proportion of non-monotonic cells (12.9 %, $n = 136$), and a slight decrease in the total percentage of monotonic cells (23.6 + 33.3 %, $n = 249 + 351$).

These differences could reflect a straightforward redistribution of response profiles or could also involve alterations in the magnitude of sound-evoked activity within each profile. To address this, we analyzed baseline-corrected sound-evoked activity across the major cell-type groups: enhanced cells (saturated + high-threshold), non-monotonic cells, and suppressed cells. Our results revealed an overall increase in absolute activity across all groups in MTHFR-deficient mice. Specifically, enhanced and non-monotonic cells showed higher sound-evoked activity (Fig. 2b left and right; 2-way ANOVA, group, enhanced cells $F = 73.8$, $p = 1 \times 10^{-17}$ and non-monotonic $F = 7.3$, $p = 0.006$), whereas suppressed cells displayed reduced activity (Fig. 2b bottom; 2-way ANOVA, group, $F = 44.1$, $p = 3.7 \times 10^{-11}$). Together these results demonstrate that the elevated baseline activity did not dampen sound-evoked responses. On the contrary, sound-evoked activity was significantly heightened, even after accounting for changes in baseline activity. Indicates that, even in a heightened state, the auditory cortex not only retains its responsiveness to stimuli but also demonstrates increased sensitivity and a significant redistribution of response profiles.

2.3. Increased inhibitory activity in MTHFR-deficient mice

To investigate the potential mechanisms driving these shifts in activity, we considered whether the reduction in suppressed cells might be linked to changes in inhibitory cell activity. If suppressed cells are primarily inhibitory, their reduced activity could account for the increased activity observed in enhanced and non-monotonic cells. Alternatively, if suppressed cells are not predominantly inhibitory, their decreased activity might serve as a compensatory mechanism to balance the heightened activity in enhanced cells. To differentiate between these possibilities, we identified sound-responsive inhibitory cells by their td-Tomato expression and analyzed their activity patterns. We found that inhibitory cell activity was predominantly enhanced rather than suppressed (Fig. 3a 2-way ANOVA, group, $F = 11.3$, $p = 0.0008$). To further investigate this phenomenon, we examined the percentage of suppressed inhibitory cells on a per-mouse basis. Suppressed cells did not constitute the majority of the inhibitory cells, and there was no significant difference in the percentage of suppressed inhibitory cells between WT and MTHFR-deficient mice (Fig. 3b *t*-test $p = 1$ corrected for multiple comparisons).

Since we are comparing PV-expressing inhibitory cells in WT mice, which constitute 40–50 % of all inhibitory neurons (Tamamaki et al., 2003; Rudy et al., 2011; Rupert and Shea, 2022; Cauli et al., 1997; Markram et al., 2004; Druga et al., 2023), to GAD-expressing inhibitory cells in MTHFR-deficient mice, the total number of suppressed inhibitory cells in WT mice would likely be higher if all inhibitory neurons were considered rather than just PV cells. To address this, we tested a new group of mice—WT-offspring from WT-mothers ($N = 3$ mice)—which, like the MTHFR-deficient mice, also expressed td-Tomato in GAD-expressing inhibitory cells. In this direct comparison, we again found no significant difference in the percentage of suppressed inhibitory cells between WT and MTHFR-deficient mice (Fig. 3b; *t*-test between MTHFR and WT2, $p = 0.7$, corrected for multiple comparisons). Additionally, we assessed whether MTHFR deficiency affects the overall proportion of GAD-expressing inhibitory cells and found no significant difference between MTHFR-deficient and WT mice (Supp Fig. 1, t-test $p = 0.56$).

2.4. Altered loudness perception and impaired sound intensity discrimination in MTHFR-deficient mice

Such changes in the inhibitory population - heightened inhibitory neural activity, coupled with an increased fraction of suppressed excitatory neurons - could act as a compensatory mechanism to maintain overall network balance, thereby preventing drastic shifts in loudness perception. On the other hand, the increased baseline activity, elevated proportion of sound-responsive neurons, and amplified responses in enhanced cells could cause changes in loudness perception, potentially causing sounds to be perceived as louder or more intrusive.

To test whether this homeostatic response is robust enough to fully counteract the heightened excitatory drive —or whether these cortical changes ultimately manifest as altered loudness perception— we employed a PSTH-based classifier to decode sound intensity from single-trial ensemble activity in the ACtx (Clayton et al., 2024; Chambers et al., 2016) (see Methods). In these analyses, confusion matrices were used to illustrate how stimulus identity was assigned based on firing patterns in ACtx units, with correct classifications falling along the upward diagonal.

By training the population activity rate decoder on trial data from enhanced cells in WT mice and then decoding the sound level on individual trials for both WT and MTHFR-deficient mice, we were able to compare their respective loudness perception. As expected, the ensemble activity in WT mice accurately, albeit not perfectly (Clayton et al., 2024; Chambers et al., 2016), predicted stimulus intensity (Fig. 4a left). On the other hand, MTHFR-deficient mice ensemble activity consistently predicted higher sound levels than those played or predicted by WT mice (Fig. 4a right), leading to lower F1 scores and higher prediction errors (Fig. 4a bottom; Permutation test *p*-value<0.001 and absolute Cohen's d effect size>2 for levels 30 to 80). For example, sounds at 60 dB were frequently classified as being 80 dB by ensemble activity in MTHFR-deficient mice.

Next, we examined whether the increased fraction of suppressed excitatory cells could compensate for the apparent hyper-sensitivity in

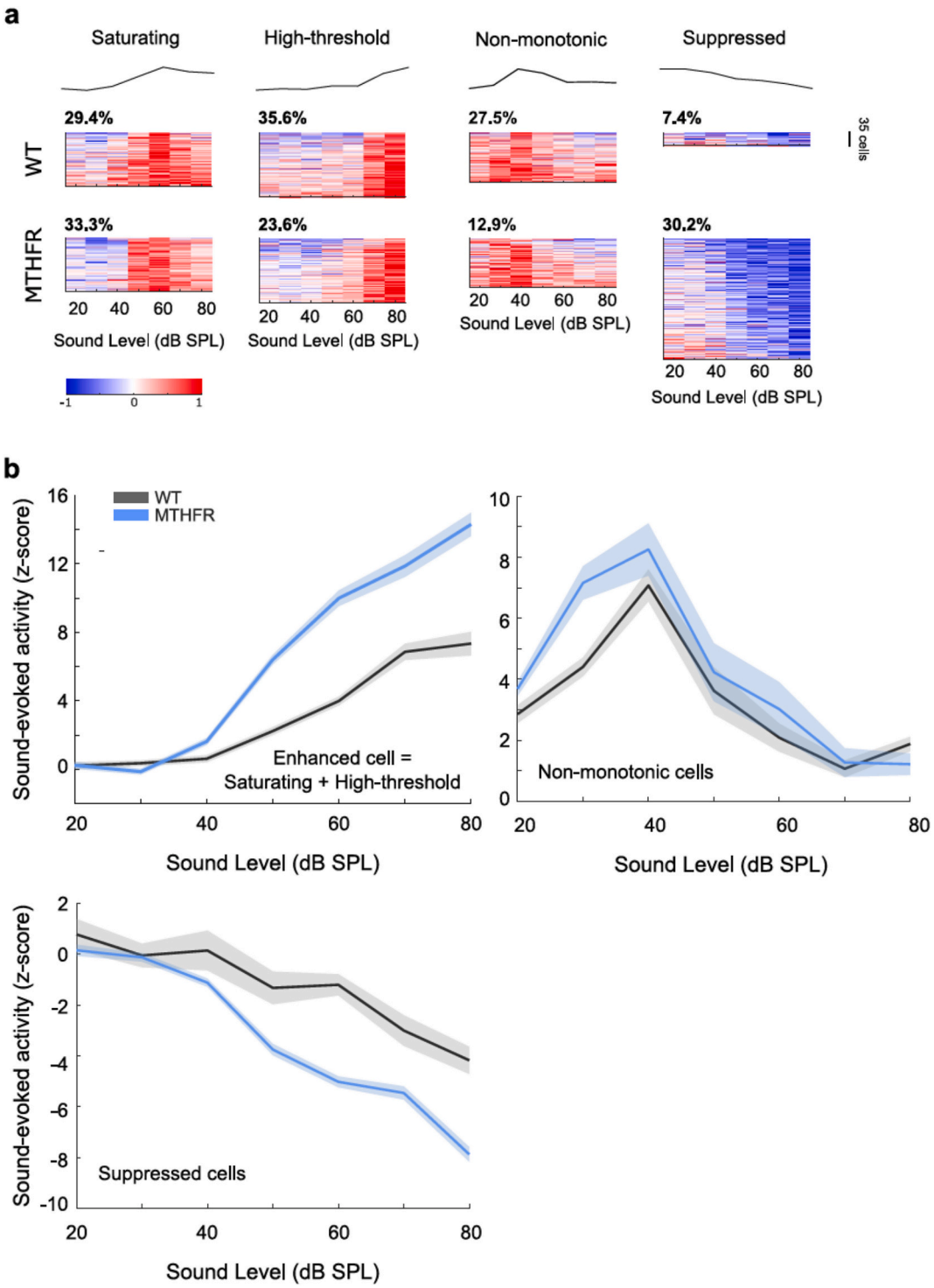

Fig. 2. Altered sound-level response profiles and increased sound-evoked activity in MTHFR-deficient mice

(a) Neurograms depict normalized, baseline-corrected activity for WT ($n = 472$) and MTHFR ($n = 1054$) sound-responsive units from 4 WT and 5 MTHFR-deficient mice in response to broadband noise of varying intensity. K-means clustering of all cells together identified four distinct response profiles that can be described as saturating (29.4 % $n = 139$, MTHFR 33.3 % $n = 351$), high-threshold (35.6 % $n = 168$, MTHFR 23.6 % $n = 249$), suppressed (7.4 % n = 35, MTHFR 30.2 % $n = 318$), and nonmonotonic (WT 27.5 % $n = 130$, MTHFR 12.9 % $n = 136$). MTHFR-deficient mice exhibited a significantly altered distribution profile from WT mice (chi2 = 141.3 $p = 1.8 \times 10^{-30}$).

(e) Sound-evoked activity at different sound intensities for enhanced, non-monotonic, and suppressed cells (mean ± se). Absolute sound-evoked activity was enhanced for all cell types (2-way ANOVA, group, enhanced cells F = 73.8, p = 1×10^{-17}, non-monotonic F = 7.3, $p = 0.006$ and suppressed cells F = 44.1, $p = 3.7 \times 10^{-11}$). Data are represented as mean ± se.

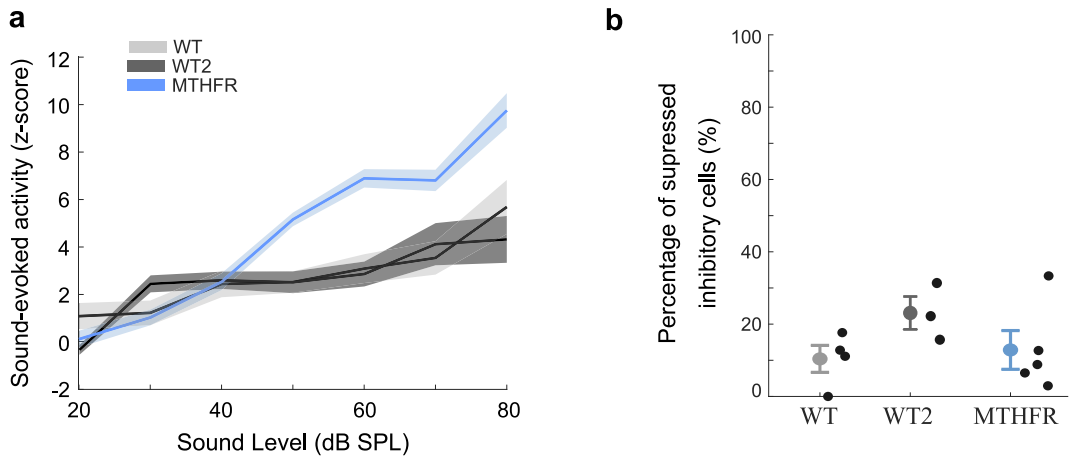

Fig. 3. Increased inhibitory activity in MTHFR-deficient mice
(a) We identified sound-responsive inhibitory cells by their expression of td-Tomato and analyzed their activity. Sound-evoked activity of inhibitory cells was stronger in MTHFR mice when compared to both of the WT groups (WT $n = 69$, MTHFR $n = 201$, 2-way ANOVA, group, $F = 11.3$, $p = 0.0008$ and WT2 (WT-offspring from WT-mothers) $n = 249$, 2-way ANOVA, group, $F = 12.1$, $p = 0.0005$, mean ± se)
(b) There was no significant difference between the percentage of inhibitory suppressed cells when comparing MTHFR mice to both WT groups (t-test $p = 0.1$ and $p = 0.7$ both corrected for multiple comparisons, mean ± se).

enhanced cells. To do this, we included both enhanced and suppressed cells in the analysis. Adding suppressed cells did not markedly alter prediction accuracy in WT mice (Fig. 4b left). However, in MTHFR-deficient mice, it significantly improved, but not completely restored, their predictive performance (Fig. 4b right; Permutation test p-value<0.001 and absolute Cohen's d effect size>2 for levels 40:60).

Changes in loudness perception may also impact the animals' ability to differentiate between sound levels, potentially altering the precision with which the auditory system detects changes in sound intensity. To test if this was the case, we simulated an intensity discrimination task by decoding ensemble responses in passively listening mice. We classified whether the mouse was presented with a 50- or 60-dB SPL noise using a binary support vector machine. In MTHFR-deficient mice, decoding accuracy was significantly lower than in WT mice (Fig. 4c left, 50 vs 60 dB SPL t-test $p = 2.3 \times 10^{-06}$). A similar reduction in accuracy was observed when testing 60 vs 70 dB SPL (Fig. 4c right, t-test $p = 4.5 \times 10^{-06}$).

These findings collectively suggest that, while the increased proportion of suppressed cells partially offsets the heightened excitatory drive in MTHFR-deficient mice, their auditory cortical activity still perceives sound intensities as higher than they are and demonstrates reduced precision in differentiating between sound levels, pointing to altered loudness perception and impaired intensity discrimination.

3. Discussion

Our findings provide compelling evidence that impaired folate metabolism, as modeled by MTHFR deficiency, leads to significant alterations in auditory cortical function. Using calcium imaging of auditory cortex neurons in vivo, we revealed atypical sound processing, characterized by increased spontaneous (Fig. 1) and sound-evoked activity (Fig. 2), shifts in response profile distributions (Fig. 2), and altered sound intensity encoding (Fig. 4). These results underscore a mechanism that may contribute to sensory hypersensitivity, a phenomenon frequently reported in atypical neurodevelopment (Sohal and Rubenstein, 2019).

MTHFR is a critical enzyme in the one-carbon metabolic pathway, essential for DNA and histone methylation. The MTHFR 677C > T polymorphism reduces enzymatic efficiency, impairing methyl group production and adversely affecting gene expression and neurodevelopment (Goin-Kochel et al., 2009; Liu et al., 2011; Pu et al., 2013; Mohammad et al., 2009). In animal models, MTHFR deficiency leads to molecular disruptions, including DNA hypomethylation and altered inhibitory dynamics, which may underlie various sensory and behavioral abnormalities (Sadigurschi and Golan, 2019; Chen et al., 2001; Sadigurschi et al., 2023; Gal et al., 2023; Shekel et al., 2021).

Examining auditory cortical function in MTHFR-deficient mice allowed us to explore how disrupted folate metabolism influences sound processing. Notably, we observed elevated baseline activity, indicative of a hyperexcitable state. Elevated baseline activity can often interfere with the auditory cortex's ability to accurately detect and process auditory stimuli, potentially leading to diminished signal-to-noise ratios. However, this was not the case here: sound-evoked activity was also significantly heightened, even after accounting for changes in baseline activity. This pattern suggests a cortex that exhibits heightened sensitivity, which may make it challenging for the system to modulate responses to auditory inputs appropriately.

In the auditory cortex, specific sound stimuli, such as white noise, can elicit diverse neural responses, including enhancement, suppression, or no response at all (Clayton et al., 2024; Wu et al., 2006; Phillips et al., 1995; Schreiner et al., 1992; Sutter and Schreiner, 1995). Among the neurons whose firing rates increase in response to sound, two primary patterns of response-level curves emerge with varying sound pressure levels. Monotonic responses steadily increase with sound intensity, while nonmonotonic responses peak at a specific sound intensity and decline thereafter (Clayton et al., 2024; Wu et al., 2006; Phillips et al., 1995; Schreiner et al., 1992; Sutter and Schreiner, 1995; Watkins and Barbour, 2011). In contrast, neurons that exhibit suppression respond to sound with a decrease firing rate relative to baseline activity. We found a marked shift in the distribution of these response profiles in MTHFR-deficient mice, with a significant decrease in the percentage of non-monotonic cells and an increase in the percentage of suppressed cells.

The impact of an increased proportion of suppressed cells largely depends on whether these cells are excitatory or inhibitory. If inhibitory cells were predominantly suppressed, it could lead to unregulated excitatory activity and network hyperexcitability. However, this does not appear to be the case in MTHFR-deficient mice. Our results suggest that suppressed cells are primarily excitatory, indicating a potential compensatory mechanism. The stronger suppression of a larger proportion of the cell population may reflect the network's attempt to offset the heightened sound-evoked activity observed in enhanced cells, thereby maintaining overall balance. Similar compensatory plasticity has been observed in other sensory systems and disorders, where shifts in inhibitory and excitatory dynamics serve to restore balance under

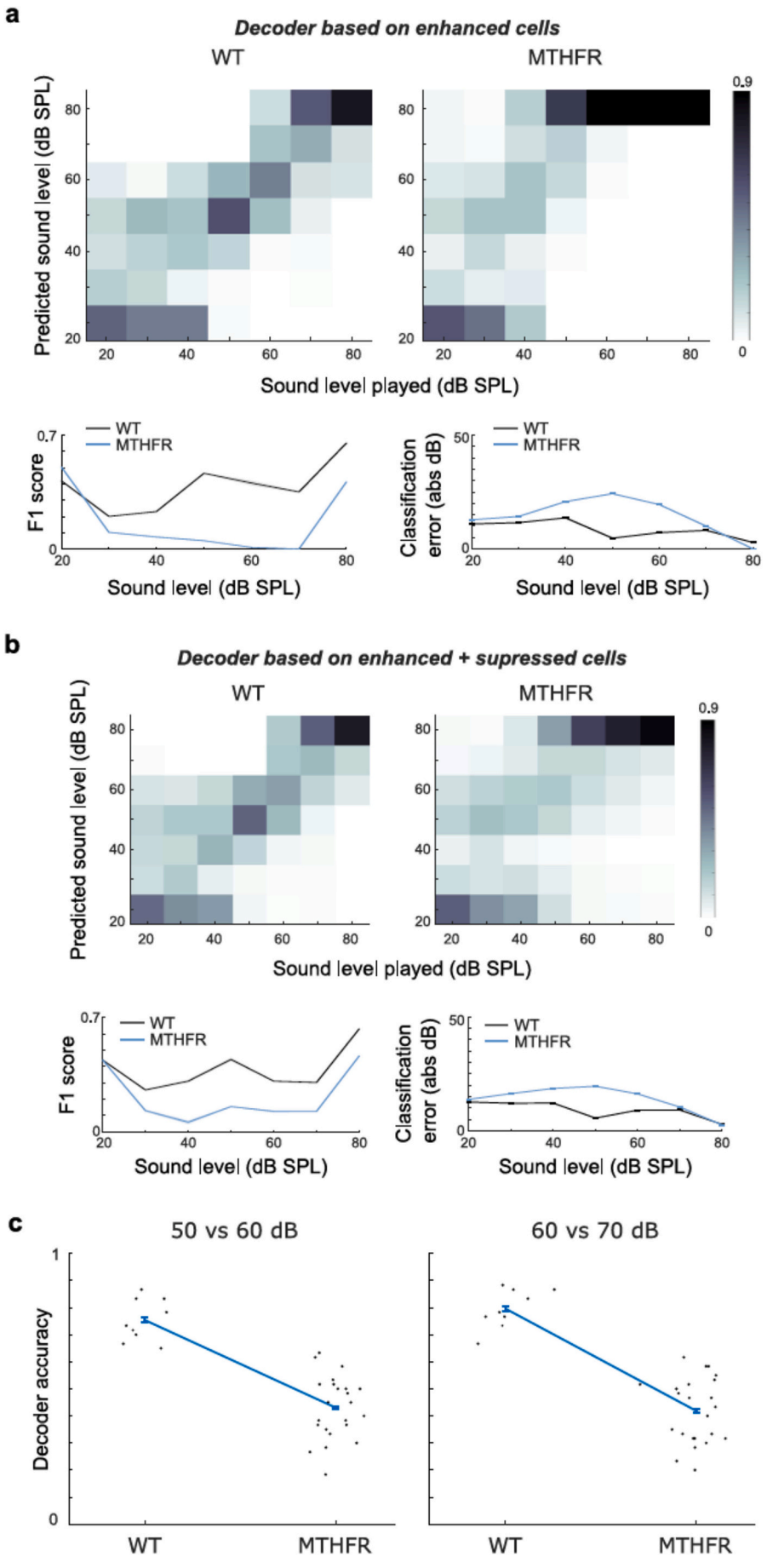

(caption on next page)

Fig. 4. Altered loudness perception and impaired sound intensity discrimination in MTHFR-deficient mice
(a) Confusion matrices for single trial PSTH-based classification of sound level by cortical activity. We trained a PSTH-based classifier to decode sound intensity from single-trial activity. For each trial, the population activity on the held-out trial was compared to the mean population activity across all sound intensities in the training set, and the classified stimulus was defined as the one with the most similar population activity. The decoder was trained with WT-enhanced cell activity, and then the sound level of individual trials was decoded from the activity of WT and MTHFR-deficient mice. Confusion matrices depict the decoding accuracy for the different sound intensities. The population activity in WT mice accurately predicted stimulus intensity, while there was an increase in loudness perception in MTHFR-deficient mice (right). Bottom: F1-score, a performance metric that evaluates the balance between precision and recall (left), and classification error comparison (right) between WT and MTHFR-deficient mice across sound intensities. Sound level identification was damaged in MTHFR mice, shown as higher predicted levels, lower F1 scores, and higher classification error (Permutation test p-value<0.001 and absolute Cohen's d effect size>2 for levels 30 to 80, mean ± se).
(b) As per (a) but including both enhanced and suppressed cells in the decoder. Adding the suppressed cells improved the sound decoding by MTHFR population activity (right) but was insufficient to fully restore sound prediction abilities to WT levels (Permutation test p-value<0.001, absolute Cohen's d effect size>2 for levels 40:60, mean ± se).
(c) We simulated an intensity discrimination task by decoding ensemble responses in passively listening mice. We classified whether the mouse was presented with a 50- or 60-dB SPL noise using a binary support vector machine. In MTHFR mice, decoding accuracy was significantly lower than in WT mice (left, 50 vs 60 dB SPL t-test $p = 2.3 \times 10^{-06}$). A similar reduction in accuracy was observed when testing 60 vs 70 dB SPL (right, t-test $p = 4.5 \times 10^{-06}$). Data are represented as mean ± se.

pathological conditions (Turrigiano, 1999; Turrigiano, 2008). For example, in visual cortical circuits, homeostatic synaptic scaling and altered excitatory/inhibitory drive can help preserve functional stability following sensory deprivation or injury (Hengen et al., 2013; Miska et al., 2018; Wu et al., 2020; Keck et al., 2011).

Neurons with nonmonotonic rate-level functions play a crucial role in encoding sound intensity, providing essential information for vocal communication (Sutter and Schreiner, 1995; Watkins and Barbour, 2011; Barbour, 2011; Watkins and Barbour, 2008; Pfingst and O'Connor, 1981). Their tuning allows for precise adaptation to prolonged or repeated stimuli and enables the auditory system to detect subtle changes in sound intensity (Wu et al., 2006; Pfingst and O'Connor, 1981; Sadagopan and Wang, 2008). While these neurons contribute to stimulus-level discrimination, the most accurate sound-level decoding arises from a combination of monotonic and nonmonotonic neurons. Nonmonotonic neurons enhance accuracy only when they constitute a significant proportion of the population, acting to complement rather than replace monotonic neurons (Sun et al., 2017).

MTHFR deficiency, through its effects on DNA and histone methylation, could impair the expression of genes involved in the formation or stabilization of synaptic connections that shape nonmonotonic tuning. Additionally, MTHFR-deficient mice exhibit decreased levels of GAD65/67 and VGAT proteins (Orenbuch et al., 2019)—key components of GABAergic signaling—that may reduce GABA release and inhibitory synaptic input. Interestingly, despite these reductions, our data shows that inhibitory neurons in MTHFR-deficient mice exhibit higher activity than WT mice. This suggests that while inhibitory neurons become more active—possibly as a compensatory response—their limited GABA production and release capacity may still lead to a net decrease in inhibition, ultimately tilting the circuit toward hyperexcitability and overshadowing the finely tuned responses typical of nonmonotonic neurons.

A reduction in non-monotonic cells diminishes the network's capacity to regulate and fine-tune responses to different sound levels. Without adequate non-monotonic cells providing inhibitory feedback at higher intensities, excitatory activity increases unchecked, leading to an overall elevation in activity. This lack of modulation dampens the system's ability to adapt to changes in sound intensity, potentially impairing loudness perception. Such alterations could hinder the ability to discern differences in loudness, posing challenges for normal speech processing or environmental sound detection.

To test if this was the case, we employed a PSTH-based classifier to decode sound levels based on ensemble activity in both WT and MTHFR-deficient mice. We found that the enhanced population activity in MTHFR-deficient mice misclassified mid- and high-level sound intensities as louder than in WT mice. Interestingly, in MTHFR-deficient mice, the heightened activity of inhibitory cells—along with an increased proportion of suppressed cells whose reduced activity and higher prevalence are likely driven by this elevated inhibition—points to a potential compensatory mechanism for stabilizing loudness perception. Indeed, a recent study showed that activating parvalbumin inhibitory cells in the auditory cortex led WT mice to classify sounds as quieter than they actually were and restored sound-level categorization to baseline values in a cochlear sensorineural hearing loss model (Clayton et al., 2024). Our analysis suggests that this compensatory mechanism operates at least partially in MTHFR-deficient mice, as including these suppressed cells in the decoder improved their loudness perception accuracy. Nevertheless, despite this improvement, the population activity in MTHFR-deficient mice continued to misclassify high-level sound intensities as somewhat louder than they actually were.

The findings in MTHFR-deficient mice, including heightened auditory cortical activity, altered response profiles, and impaired sound-level discrimination, align closely with sensory hypersensitivity observed in individuals with ASD (Schulz and Stevenson, 2019). Human studies frequently report that individuals with ASD experience discomfort in noisy environments and difficulty distinguishing between sound levels, both of which are hallmarks of altered auditory processing (Griffiths, 2002; de Wit et al., 2016). Enhanced neural responses to auditory stimuli, such as increased amplitude of auditory evoked potentials, have been consistently observed in ASD and are thought to underlie heightened sensitivity to environmental sounds (Khalfa et al., 2004; Wiggins et al., 2009; Bishop and Seltzer, 2012; Poulsen et al., 2024). Given that MTHFR deficiency is associated with an elevated risk of ASD (Boris and Galanko, 2004; Goin-Kochel et al., 2009; Pu et al., 2013; Mohammad et al., 2009; de Wit et al., 2016), the observed shift in response profiles and increased suppression could help explain the broad range of auditory sensitivities found in ASD: reduced filtering by nonmonotonic neurons may drive hypersensitivity in some individuals, while excessive compensatory suppression might lead to hypo-responsiveness in others.

The altered loudness perception observed in MTHFR-deficient mice could have significant everyday implications for humans carrying this deficiency. Overestimation of sound intensities might lead to heightened avoidance of environmental sounds or difficulty discriminating between critical auditory cues, such as those needed for communication or detecting potential threats. Such deficits could impair their ability to navigate social and physical environments, or adapt to changing auditory contexts, potentially mirroring challenges observed in many neurodevelopmental disorders. Future research might explore whether restoring folate-dependent methylation can rescue abnormal synaptic and circuit dynamics in MTHFR-deficient mice, and whether such interventions improve their atypical acoustic processing. Additionally, longitudinal studies could assess whether these auditory phenotypes emerge early in development or reflect compensatory adaptations that evolve over time. Such insights might inform preventative or therapeutic strategies for individuals carrying MTHFR deficiencies, including those at risk for ASD or other neurodevelopmental disorders characterized by atypical sensory processing.

4. Methods

4.1. Experimental model and subject details

All procedures were approved by the Ben-Gurion University animal care and use. Data was collected from 12 adult mice (8–16 weeks postnatal).

MTHFR-deficient mice were created by mating Mthfr +/− (HT) (Chen et al., 2001) females with Balb/cAnNCrlBR background with GAD65-tdTomato males with C57/Bl6 BAC background (Besser et al., 2015). We found no differences between WT offspring from MTHFR-deficient mothers (HT: WT) (N = 1 mouse) and MTHFR-deficient offspring from MTHFR-deficient mothers (HT: HT) (N = 4 mice) on the variables measured in this study, so we combined their results. PV-Cre x Ai14 mice (N = 4, JAX stock no: 017320 and 024109, respectively) and WT offspring from Mthfr +/+ mothers (N = 3) were used as controls. Mice of both sexes were used for this study. We found no differences in the variables measured in this study between males and females. Mice were maintained on a reverse 12 h light/12 h dark cycle and provided ad libitum access to food and water.

4.2. Survival surgeries for awake, head-fixed imaging and behavior experiments

Mice were anesthetized with isoflurane in oxygen (5 % induction, 1.5 % maintenance). The dorsal surface of the mice's heads was trimmed and sterilized. ThermoStar homeothermic blanket monitoring system was used to maintain body temperature at 36.6C° (RWD). Lidocaine hydrochloride was administered subcutaneously to numb the scalp. The dorsal surface of the scalp was reduced using surgical scissors, and the periosteum was removed. The skull surface was prepped with an etchant (C&B metabond) and vetbond (3 M) before affixing a custom stainless-steel headplate to the dorsal surface with dental cement (C&B metabond). At the conclusion of the headplate attachment and any additional procedures listed below, Buprenex (0.05 mg/kg) and meloxicam (0.1 mg/kg) were administered, and the animal was transferred to a warmed recovery chamber.

4.3. Virus mediated gene-delivery

For mice used in imaging experiments, two burr holes were made in the skull over the auditory cortex (1.75–2.25 mm rostral to the lambdoid suture). A precision injection system (Nanoject III) was used to inject 75 nL of AAV5.Syn.GCaMP6s.WPRE.SV40 in each burr hole 200-250 mm below the pial surface. Before starting the imaging sessions, we waited ~3 weeks for virus incubation.

4.4. Two-photon calcium imaging

Three round glass coverslips (one 4 mm, two 3 mm, #1 thickness) were etched with piranha solution and bonded into a vertical stack using transparent, UV-cured adhesive. Headplate attachment, anesthesia and analgesia follow the procedure described above. A 3 mm craniotomy was made over the right ACtx using a scalpel and the coverslip stack was cemented into the craniotomy. An initial widefield epifluorescence imaging session was performed to visualize the tonotopic gradients of the auditory cortex and identify the position of A1 as described previously (Chambers et al., 2016; Romero et al., 2025; Kazanovich et al., 2024). Two-photon excitation was provided by a Ti:Sapphire-pulsed laser tuned to 920 nm. Imaging was performed with a 16 X/0.8NA water-immersion objective (Nikon) from a 512 × 512 pixel field of view at 30 Hz with a Galvo-Resonant 8 kHz scanning microscope (Thorlabs). Scanning software was synchronized to the stimulus generation hardware using digital pulse trains. The microscope was rotated 50–60 degrees off the vertical axis to obtain images from the lateral aspect of the mouse cortex while the animal was maintained in an upright head position. Imaging was performed in a light-tight, sound-attenuating chamber mounted on a floating table. Animals were monitored throughout the experiment to confirm that all imaging was performed in the awake condition. Imaging was performed in layers L2/3, 200–230 mm below the pial surface. Each session we returned to the same area, guided by the blood vasculature, but not necessarily the same cells. Fluorescence images were captured at 2× digital zoom, providing an imaging field of (0.42 × 0.42 mm). Raw calcium movies were processed using Suite2P (Pachitariu et al., 2017), a publicly available two-photon calcium imaging analysis pipeline. ΔF/F was computed as follows: (F(t)- F0)/F0, where F(t) was the raw calcium signal and F0 was the mean baseline fluorescence before stimulus presentation across trials. Spike deconvolution was also performed in Suite2P (Pachitariu et al., 2017), using the default method based on the OASIS algorithm (Pachitariu et al., 2018; Pachitariu et al., 2017; Stringer and Pachitariu, 2019). All analyses were performed using ΔF/F except the calculation of baseline activity in Fig. 1, which was performed using deconvolved activity.

4.5. Auditory stimulus for imaging experiments

Auditory stimuli were generated with a 24-bit digital-to-analog converter (National Instruments model PXI-4461) using scripts programmed in MATLAB (MathWorks) and LabVIEW (National Instruments). Speakers were calibrated for their distance from the mouse's contralateral ear (left ear). For imaging experiments, we played a 100 ms white noise generated from a Gaussian distribution at different sound intensities (20–80 dB SPL with 10 dB SPL step. All the trials had a 3-s duration. Each stimulus was repeated 30 times.

4.6. Two-photon calcium imaging analysis

Baseline activity: was calculated as average deconvolved spike activity in the second preceding sound onset.

Rate-level functions: A unit was classified as sound-responsive if a nonparametric Wilcoxon signed-rank test revealed significant differences in trial-by-trial activity between the 350 ms period before and after stimulus onset (calculated per sound level). To meet the criteria for sound responsiveness, the post-stimulus activity had to differ significantly from the pre-stimulus activity for at least two sound levels. Rate level functions were computed for all sound-responsive units by calculating the z-score values of the activity post-stimulus. For visualization and clustering, rate-level functions were normalized to their absolute maximum values. K-means clustering was performed on all sound-responsive units in Matlab using the "kmeans" function (maximum iterations, 1000; replicates, 10; distance metric, correlation).

Analysis of inhibitory cells: We identified inhibitory cells in the first WT mice groupu as PV-expressing cells and in the second WT group and MTHFR-deficient mice as GAD-expressing cells, based on td-Tomato expression. Following identification, we determined the sound-responsive cells among these inhibitory populations and assigned them to their respective k-means clusters. Finally, we calculated the percentage of inhibitory cells that were part of the suppressed cluster.

Loudness classification: we performed population-based classification of sound levels using ΔF/F activity recorded during the 500 ms following stimulus onset. For the analysis in Fig. 4a, the classifier was trained using 150 randomly selected enhanced units from WT mice; for Fig. 4b, 150 randomly selected units were drawn from the combined pool of enhanced and suppressed WT units. For each sound level, the population activity of the held-out trial was compared to the mean population activity across all stimuli in the training set, and the trial was classified as belonging to the stimulus with the most similar population activity (Miska et al., 2018). Classification was performed iteratively, with each trial serving as the held-out test trial (leave-one-out cross-validation). Overall classification accuracy was averaged over 1000 random draws of units. To compare loudness perception between WT and MTHFR-deficient mice, MTHFR trials were decoded using the

classifier trained on WT data.

Sound level discrimination: We employed a linear kernel Support Vector Machine (SVM) classifier to determine how ensemble activity decoded the different noise levels. This classifier model was trained using a data matrix of cell activity. The data matrix was comprised of the average sound evoked activity within a 500 ms window after the stimulus onset normalized by the pre-stimulus activity. Ensemble analysis included all cells per session. We employed k-fold cross-validation method ($k = 10$) to train the classifier and compute the misclassification rate on untrained trials (we got the same results with leave-one-out cross-validation). We replicated this procedure independently for each mouse and imaging session, ultimately calculating the mean decoding accuracy across sessions. The SVM training and cross-validation procedure were executed in MATLAB, utilizing the 'fitcsvm,' 'crossval,' and 'kfoldLoss' functions.

4.7. Statistical analysis

All statistical analyses were performed in MATLAB R2023a (Mathworks). Data shown in all analyses is the mean activity ± SE unless otherwise indicated. Post hoc pairwise comparisons were corrected for multiple comparisons using the Bonferroni correction.

CRediT authorship contribution statement

Hila Sapir: Formal analysis, Data curation. **Ghattas Bisharat:** Data curation. **Hava Golan:** Writing – review & editing, Resources. **Jennifer Resnik:** Writing – review & editing, Writing – original draft, Supervision, Funding acquisition, Conceptualization.

Declaration of competing interest

The authors declare the following financial interests/personal relationships which may be considered as potential competing interests:

Jennifer Resnik reports financial support was provided by Israel Science Foundation. If there are other authors, they declare that they have no known competing financial interests or personal relationships that could have appeared to influence the work reported in this paper.

Acknowledgments

This research was supported by the ISRAEL SCIENCE FOUNDATION (grant No. 725/21) and the National Institute for Psychobiology in Israel. We thank Ken Hancock for his support and technical brilliance, Danielle Barda for the breeding and genotyping of the mice, and the Resnik Lab for comments on this work.

Appendix A. Supplementary data

Supplementary data to this article can be found online at https://doi.org/10.1016/j.nbd.2025.106863.

Data availability

The source data of this paper is available upon request to resnikj@bgu.ac.il.

References

Agam, G., Taylor, Z., Vainer, E., Golan, H.M., 2020. The influence of choline treatment on behavioral and neurochemical autistic-like phenotype in Mthfr-deficient mice. Transl. Psychiatry 10, 316. https://doi.org/10.1038/s41398-020-01002-1.

Barbour, D.L., 2011. Intensity-invariant coding in the auditory system. Neurosci. Biobehav. Rev. 35, 2064–2072. https://doi.org/10.1016/j.neubiorev.2011.04.009.

Besser, S., Sicker, M., Marx, G., Winkler, U., Eulenburg, V., Hülsmann, S., et al., 2015. A transgenic mouse line expressing the red fluorescent protein tdTomato in GABAergic neurons. PLoS One 10, e0129934. https://doi.org/10.1371/journal.pone.0129934.

Bishop, S.L., Seltzer, M.M., 2012. Self-reported autism symptoms in adults with autism spectrum disorders. J. Autism Dev. Disord. 42, 2354–2363. https://doi.org/10.1007/s10803-012-1483-2.

Boris, M., Galanko, J., 2004. Association of MTHFR Gene Variants with Autism, p. 9.

Cauli, B., Audinat, E., Lambolez, B., Angulo, M.C., Ropert, N., Tsuzuki, K., et al., 1997. Molecular and physiological diversity of cortical nonpyramidal cells. J. Neurosci. 17, 3894–3906. https://doi.org/10.1523/JNEUROSCI.17-10-03894.1997.

Chambers, A.R., Resnik, J., Yuan, Y., Whitton, J.P., Edge, A.S., Liberman, M.C., et al., 2016. Central gain restores auditory processing following near-complete cochlear denervation. Neuron 89, 867–879. https://doi.org/10.1016/j.neuron.2015.12.041.

Chen, Z., Karaplis, A.C., Ackerman, S.L., Pogribny, I.P., Melnyk, S., Lussier-Cacan, S., et al., 2001. Mice deficient in methylenetetrahydrofolate reductase exhibit hyperhomocysteinemia and decreased methylation capacity, with neuropathology and aortic lipid deposition. Hum. Mol. Genet. 10, 433–444. https://doi.org/10.1093/hmg/10.5.433.

Clayton, K.K., McGill, M., Awwad, B., Stecyk, K.S., Kremer, C., Skerleva, D., et al., 2024. Cortical determinants of loudness perception and auditory hypersensitivity. bioRxiv. https://doi.org/10.1101/2024.05.30.596691, p. 2024.05.30.596691.

de Wit, E., Visser-Bochane, M.I., Steenbergen, B., van Dijk, P., van der Schans, C.P., Luinge, M.R., 2016. Characteristics of auditory processing disorders: a systematic review. J. Speech Lang. Hear. Res. 59, 384–413. https://doi.org/10.1044/2015_JSLHR-H-15-0118.

Druga, R., Salaj, M., Al-Redouan, A., 2023. Parvalbumin - positive neurons in the neocortex: a review. Physiol. Res. 72, S173–S191. https://doi.org/10.33549/physiolres.935005.

Feng, L., Song, Z., Xin, F., Hu, J., 2009. Association of plasma homocysteine and methylenetetrahydrofolate reductase C677T gene variant with schizophrenia: a Chinese Han population-based case–control study. Psychiatry Res. 168, 205–208. https://doi.org/10.1016/j.psychres.2008.05.009.

Frosst, P., Blom, H.J., Milos, R., Goyette, P., Sheppard, C.A., Matthews, R.G., et al., 1995. A candidate genetic risk factor for vascular disease: a common mutation in methylenetetrahydrofolate reductase. Nat. Genet. 10, 111–113. https://doi.org/10.1038/ng0595-111.

Gal, A., Raykin, E., Giladi, S., Lederman, D., Kofman, O., Golan, H.M., 2023. Temporal dynamics of isolation calls emitted by pups in environmental and genetic mouse models of autism spectrum disorder. Front. Neurosci. 17, 1274039. https://doi.org/10.3389/fnins.2023.1274039.

Goin-Kochel, R.P., Porter, A.E., Peters, S.U., Shinawi, M., Sahoo, T., Beaudet, A.L., 2009. The MTHFR 677C→T polymorphism and behaviors in children with autism: exploratory genotype–phenotype correlations. Autism Res. 2, 98–108. https://doi.org/10.1002/aur.70.

Griffiths, T.D., 2002. Central auditory processing disorders. Curr. Opin. Neurol. 15, 31.

Hengen, K.B., Lambo, M.E., Van Hooser, S.D., Katz, D.B., Turrigiano, G.G., 2013. Firing rate homeostasis in visual cortex of freely behaving rodents. Neuron 80. https://doi.org/10.1016/j.neuron.2013.08.038.

Kazanovich, I., Itzhak, S., Resnik, J., 2024. Experience-driven development of decision-related representations in the auditory cortex. EMBO Rep. 26, 84–100. https://doi.org/10.1038/s44319-024-00309-0.

Keck, T., Scheuss, V., Jacobsen, R.I., Wierenga, C.J., Eysel, U.T., Bonhoeffer, T., et al., 2011. Loss of sensory input causes rapid structural changes of inhibitory neurons in adult mouse visual cortex. Neuron 71, 869–882. https://doi.org/10.1016/j.neuron.2011.06.034.

Khalfa, S., Bruneau, N., Rogé, B., Georgieff, N., Veuillet, E., Adrien, J.-L., et al., 2004. Increased perception of loudness in autism. Hear. Res. 198, 87–92. https://doi.org/10.1016/j.heares.2004.07.006.

Levine, S.Z., Kodesh, A., Viktorin, A., Smith, L., Uher, R., Reichenberg, A., et al., 2018. Association of maternal use of folic acid and multivitamin supplements in the periods before and during pregnancy with the risk of autism spectrum disorder in offspring. JAMA Psychiatr. 75, 176–184. https://doi.org/10.1001/jamapsychiatry.2017.4050.

Lewis, S.J., Zammit, S., Gunnell, D., Smith, G.D., 2005. A meta-analysis of the MTHFR C677T polymorphism and schizophrenia risk. Am. J. Med. Genet. B Neuropsychiatr. Genet. 135B, 2–4. https://doi.org/10.1002/ajmg.b.30170.

Liu, X., Solehdin, F., Cohen, I.L., Gonzalez, M.G., Jenkins, E.C., Lewis, M.E.S., et al., 2011. Population- and family-based studies associate the MTHFR gene with idiopathic autism in simplex families. J. Autism Dev. Disord. 41, 938–944. https://doi.org/10.1007/s10803-010-1120-x.

Markram, H., Toledo-Rodriguez, M., Wang, Y., Gupta, A., Silberberg, G., Wu, C., 2004. Interneurons of the neocortical inhibitory system. Nat. Rev. Neurosci. 5, 793–807. https://doi.org/10.1038/nrn1519.

Mattson, M.P., Shea, T.B., 2003. Folate and homocysteine metabolism in neural plasticity and neurodegenerative disorders. Trends Neurosci. 26, 137–146. https://doi.org/10.1016/S0166-2236(03)00032-8.

Miska, N.J., Richter, L.M., Cary, B.A., Gjorgjieva, J., Turrigiano, G.G., 2018. Sensory experience inversely regulates feedforward and feedback excitation-inhibition ratio in rodent visual cortex. Kauer JA, Westbrook GL, editors. eLife 7, e38846. https://doi.org/10.7554/eLife.38846.

Mohammad, N.S., Jain, J.M.N., Chintakindi, K.P., Singh, R.P., Naik, U., Akella, R.R.D., 2009. Aberrations in folate metabolic pathway and altered susceptibility to autism. Psychiatr. Genet. 19, 171. https://doi.org/10.1097/YPG.0b013e32832cebd2.

Muntjewerff, J.W., Kahn, R.S., Blom, H.J., den Heijer, M., 2006. Homocysteine, methylenetetrahydrofolate reductase and risk of schizophrenia: a meta-analysis. Mol. Psychiatry 11, 143–149. https://doi.org/10.1038/sj.mp.4001746.

Orenbuch, A., Fortis, K., Taesuwan, S., Yaffe, R., Caudill, M.A., Golan, H.M., 2019. Prenatal nutritional intervention reduces autistic-like behavior rates among Mthfr-deficient mice. Front. Neurosci. 13, 383. https://doi.org/10.3389/fnins.2019.00383.

Pachitariu, M., Stringer, Carsen, Dipoppa, Mario, Schröder, Sylvia, Rossi, L. Federico, Dalgleish, Henry, et al., 2017. Suite2p: Beyond 10,000 neurons with standard two-photon microscopy | bioRxiv. https://doi.org/10.1101/061507v2 [cited 20 Sep 2023]. Available:

Pachitariu, M., Stringer, C., Harris, K.D., 2018. Robustness of spike deconvolution for neuronal calcium imaging. J. Neurosci. 38, 7976–7985. https://doi.org/10.1523/JNEUROSCI.3339-17.2018.

Pfingst, B.E., O'Connor, T.A., 1981. Characteristics of neurons in auditory cortex of monkeys performing a simple auditory task. J. Neurophysiol. 45, 16–34. https://doi.org/10.1152/jn.1981.45.1.16.

Phillips, D.P., Semple, M.N., Kitzes, L.M., 1995. Factors shaping the tone level sensitivity of single neurons in posterior field of cat auditory cortex. J. Neurophysiol. 73, 674–686.

Poulsen, R., Williams, Z., Dwyer, P., Pellicano, E., Sowman, P.F., McAlpine, D., 2024. How auditory processing influences the autistic profile: a review. Autism Res. 17, 2452–2470. https://doi.org/10.1002/aur.3259.

Pu, D., Shen, Y., Wu, J., 2013. Association between MTHFR gene polymorphisms and the risk of autism spectrum disorders: a Meta-analysis. Autism Res. 6, 384–392. https://doi.org/10.1002/aur.1300.

Romero, S., Hight, A.E., Clayton, K.K., Resnik, J., Williamson, R.S., Hancock, K.E., 2025. et al. Cellular and Widefield Imaging of Sound Frequency Organization in Primary and Higher Order Fields of the Mouse Auditory Cortex.

Roza, S.J., van Batenburg-Eddes, T., Steegers, E.A.P., Jaddoe, V.W.V., Mackenbach, J.P., Hofman, A., et al., 2010. Maternal folic acid supplement use in early pregnancy and child behavioural problems: the generation R study. Br. J. Nutr. 103, 445–452. https://doi.org/10.1017/S0007114509991954.

Rudy, B., Fishell, G., Lee, S., Hjerling-Leffler, J., 2011. Three groups of interneurons account for nearly 100% of neocortical GABAergic neurons. Dev. Neurobiol. 71, 45–61. https://doi.org/10.1002/dneu.20853.

Rupert, D.D., Shea, S.D., 2022. Parvalbumin-positive interneurons regulate cortical sensory plasticity in adulthood and development through shared mechanisms. Front. Neural Circ. 16. https://doi.org/10.3389/fncir.2022.886629.

Sadagopan, S., Wang, X., 2008. Level invariant representation of sounds by populations of neurons in primary auditory cortex. J. Neurosci. 28, 3415–3426. https://doi.org/10.1523/JNEUROSCI.2743-07.2008.

Sadigurschi, N., Golan, H.M., 2019. Maternal and offspring methylenetetrahydrofolate-reductase genotypes interact in a mouse model to induce autism spectrum disorder-like behavior. Genes Brain Behav. 18, e12547. https://doi.org/10.1111/gbb.12547.

Sadigurschi, N., Scrift, G., Hirrlinger, J., Golan, H.M., 2023. Genetic impairment of folate metabolism regulates cortical interneurons and social behavior. Front. Neurosci. 17, 1203262. https://doi.org/10.3389/fnins.2023.1203262.

Schreiner, C.E., Mendelson, J.R., Sutter, M.L., 1992. Functional topography of cat primary auditory cortex: representation of tone intensity. Exp. Brain Res. 92, 105–122. https://doi.org/10.1007/BF00230388.

Schulz, S.E., Stevenson, R.A., 2019. Sensory hypersensitivity predicts repetitive behaviours in autistic and typically-developing children. Autism 23, 1028–1041. https://doi.org/10.1177/1362361318774559.

Shekel, I., Giladi, S., Raykin, E., Weiner, M., Chalifa-Caspi, V., Lederman, D., et al., 2021. Isolation-induced ultrasonic vocalization in environmental and genetic mice models of autism. Front. Neurosci. 15, 769670. https://doi.org/10.3389/fnins.2021.769670.

Sohal, V.S., Rubenstein, J.L.R., 2019. Excitation-inhibition balance as a framework for investigating mechanisms in neuropsychiatric disorders. Mol. Psychiatry 24, 1248–1257. https://doi.org/10.1038/s41380-019-0426-0.

Stringer, C., Pachitariu, M., 2019. Computational processing of neural recordings from calcium imaging data. Curr. Opin. Neurobiol. 55, 22–31. https://doi.org/10.1016/j.conb.2018.11.005.

Sun, W., Marongelli, E.N., Watkins, P.V., Barbour, D.L., 2017. Decoding sound level in the marmoset primary auditory cortex. J. Neurophysiol. 118, 2024–2033. https://doi.org/10.1152/jn.00670.2016.

Sutter, M.L., Schreiner, C.E., 1995. Topography of intensity tuning in cat primary auditory cortex: single-neuron versus multiple-neuron recordings. J. Neurophysiol. 73, 190–204. https://doi.org/10.1152/jn.1995.73.1.190.

Tamamaki, N., Yanagawa, Y., Tomioka, R., Miyazaki, J.-I., Obata, K., Kaneko, T., 2003. Green fluorescent protein expression and colocalization with calretinin, parvalbumin, and somatostatin in the GAD67-GFP knock-in mouse. J. Comp. Neurol. 467, 60–79. https://doi.org/10.1002/cne.10905.

Turrigiano, G.G., 1999. Homeostatic plasticity in neuronal networks: the more things change, the more they stay the same. Trends Neurosci. 22, 221–227. https://doi.org/10.1016/S0166-2236(98)01341-1.

Turrigiano, G.G., 2008. The self-tuning neuron: synaptic scaling of excitatory synapses. Cell 135, 422–435. https://doi.org/10.1016/j.cell.2008.10.008.

van der Put, N.M., Eskes, T.K., Blom, H.J., 1997. Is the common 677C–>T mutation in the methylenetetrahydrofolate reductase gene a risk factor for neural tube defects? A meta-analysis. QJM 90, 111–115.

Watkins, P.V., Barbour, D.L., 2008. Specialized neuronal adaptation for preserving input sensitivity. Nat. Neurosci. 11, 1259–1261. https://doi.org/10.1038/nn.2201.

Watkins, P.V., Barbour, D.L., 2011. Level-tuned neurons in primary auditory cortex adapt differently to loud versus soft sounds. Cereb. Cortex 21, 178–190. https://doi.org/10.1093/cercor/bhq079.

Wiggins, L.D., Robins, D.L., Bakeman, R., Adamson, L.B., 2009. Breif report: sensory abnormalities as distinguishing symptoms of autism spectrum disorders in young children. J. Autism Dev. Disord. 39, 1087–1091. https://doi.org/10.1007/s10803-009-0711-x.

Wu, G.K., Li, P., Tao, H.W., Zhang, L.I., 2006. Nonmonotonic synaptic excitation and imbalanced inhibition underlying cortical intensity tuning. Neuron 52, 705–715. https://doi.org/10.1016/j.neuron.2006.10.009.

Wu, Y.K., Hengen, K.B., Turrigiano, G.G., Gjorgjieva, J., 2020. Homeostatic mechanisms regulate distinct aspects of cortical circuit dynamics. Proc. Natl. Acad. Sci. USA 117, 24514–24525. https://doi.org/10.1073/pnas.1918368117.

Zou, R., El Marroun, H., Cecil, C., Jaddoe, V.W.V., Hillegers, M., Tiemeier, H., et al., 2021. Maternal folate levels during pregnancy and offspring brain development in late childhood. Clin. Nutr. 40, 3391–3400. https://doi.org/10.1016/j.clnu.2020.11.025.